PROCEEDINGS OF SCIENCE

Does the Local Bubble bias Galactic magnetic field models used to backtrack UHECRs?

V. Pelgrims,[a,*] **M. Unger**[b,c] **and I. C. Mariş**[a]

[a] *Université Libre de Bruxelles, Science Faculty, CP230, B-1050 Brussels, Belgium*

[b] *Institut für Astroteilchenphysik, Karlsruher Institut für Technologie, Karlsruhe 76344, Germany*

[c] *Institutt for fysikk, Norwegian University of Science and Technology (NTNU), Trondheim, Norway*

E-mail: vincent.pelgrims@ulb.be

On their journey from their source to Earth, electrically-charged cosmic rays are deflected by magnetic fields. While small-scale magnetized structures have no impact on the propagation of ultra-high-energy cosmic rays, they can have an impact on our reconstruction of the large-scale magnetic field obtained from synchrotron and Faraday rotation data. In this context, the Local Bubble, a cavity of hot gas surrounded by a thick magnetized dusty shell, is perhaps one of the most important foregrounds to consider as it surrounds us. In this work, we use a new analytical model to describe the divergence-free magnetic field in the shell of Galactic bubbles to assess the impact of the geometric characterization of the Local Bubble shell on predictions of its contribution to Galactic magnetic field observables. We show that the choice of the shape of the Local Bubble shell and the location of the explosion that has led to the formation of the bubble are important factors to consider. They are decisive in estimating the contribution of the magnetized shell of the Local Bubble to synchrotron polarized emission and Faraday rotation measures. In addition, we find that the contribution of the Local Bubble shell to synchrotron polarized emission is likely to be substantial at high Galactic latitudes. This may point to potential biases in current modeling of the large-scale Galactic magnetic field, and hence in back-propagation studies of ultra-high-energy cosmic rays. Further analysis will be required to fully ascertain the impact of this foreground.

7th International Symposium on Ultra High Energy Cosmic Rays (UHECR2024)
17-21 November 2024
Malargüe, Mendoza, Argentina

*Speaker

ISSN 1824-8039. Published by SISSA Medialab.

PoS(UHECR2024)108

1. Introduction

Knowledge about the three-dimensional (3D) structure of the Galactic magnetic field (GMF) is important to study ultra-high-energy cosmic rays (UHECR) and understand the data on arrival direction, mass composition, energy spectrum, and how they relate to propagation effects [1, 2]. To gain insight into the general structure and amplitude of the GMF on the kiloparsec scale relevant to UHECR propagation, authors have primarily relied on observations of Faraday rotation measures (RM) toward extragalactic sources and on Galactic synchrotron emission. Using forward modeling frameworks, where model predictions are compared to observations, constraints on a variety of 3D models for the GMF (see, e.g., [3] for a review and [4, 5] for the most recent updates) have been deduced. One of the main limitations of this approach is the line-of-sight-integrated nature of the observables, which leads to degeneracy between models and model parameters and consequently to uncertainties in the reconstructed picture of the GMF [4].

In this context, most efforts to model the large-scale GMF have overlooked the fact that the Solar system resides in the Local Bubble. The Local Bubble is a cavity with unusually low density of gas, filled with an X-ray emitting plasma, and surrounded by a shell of cold (ionized) gas and dust [6–10]. This local cavity has most likely been created by successive supernova explosions that occurred in the past 10-15 Myr [11–13]. As for other explosion-induced bubbles in the interstellar medium (ISM), the initial local magnetic field is expected to have been altered by supernova explosions. By dragging the frozen-in magnetic field lines with it, the explosion-induced motion of matter deformed and confined the magnetic field lines into the shell of the resulting bubble. This is supported by starlight polarization data which show that the magnetic field in the local ISM does not follow the large-scale GMF pattern and exhibits an increased amplitude in the shell of the Local Bubble [14–19]. However, the contribution of the magnetized shell of the Local Bubble to the line-of-sight-integrated observables which are sensitive to the GMF is still unknown, or at least little constrained.

Recently, the magnetized shell of the Local Bubble has been implemented in an attempt to model the coherent component of the GMF [5]. It was found that the Local Bubble contributes substantially to the Faraday RM and polarized synchrotron emission at high Galactic latitudes and, hence, has an impact on the reconstruction of the large-scale field. In the previous research, it was considered a simple spherical model to describe the Local Bubble which relied on a nonphysical prescription to model the magnetic field in its shell. In this work, we explore the impacts of going beyond this simple prescription. We consider the solenoidal solution for the magnetic field in the shell of irregularly-shaped Galactic bubbles and a more realistic shape for the Local Bubble shell which is known. From observation, the shell is known to be irregular and highly asymmetric, with a radius of about 100 pc in the Galactic plane and of about 300 pc perpendicular to it [9], as illustrated in the middle panel of Figure 1.

2. Improved model for the magnetic field in the shell of the Local Bubble

2.1 Magnetic field in irregularly-shaped Galactic bubbles

Starting from the induction equation without magnetic diffusion, we obtained the solenoidal solution for the magnetic field in the thick shells of Galactic bubbles that result from supernova

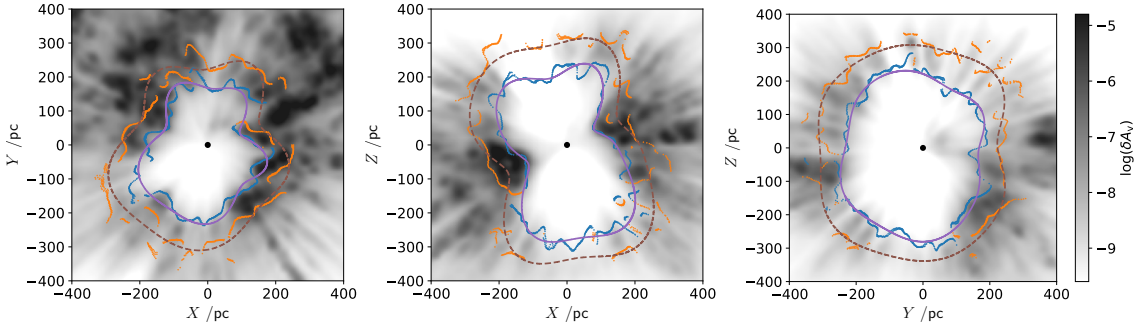

Figure 1: Crosscuts along the planes XY, XZ, and YZ in the 3D dust extinction map of [21]. We use the Heliocentric Galactic coordinates. The (common) gray scale shows $\log(\delta A_{\rm v})$, with $\delta A_{\rm v}$ the differential of the dust extinction in units of magnitude per parsec. The blue and orange dots mark the inner and outer surfaces of the Local Bubble shell measured from the radial profiles of $\delta A_{\rm v}$. The purple and brown continuous lines trace the intersections with the respective plane of our models for $r_{\rm inner}^{\ell_{\rm max}=6}$ and $r_{\rm outer}^{\ell_{\rm max}=6}$ obtained from a spherical harmonic decomposition of the measurements with a maximum multipole of 6.

explosion [20]. The model assumes a single effective explosion that induces a radial displacement of the ISM matter with respect to the explosion center, but not necessarily with spherical symmetry. According to the frozen-in approximation, the magnetic field that is assumed to be initially uniform is then perturbed by the displacement of matter. The magnetic field lines are stretched and squeezed to follow the shape of the shell of the bubble that results from the explosion. Considering a simple model for the matter displacement field, we proposed a physically satisfying solution that makes it possible to fully describe the magnetic field $\mathbf{B}$ anywhere in the shell of Galactic bubbles from the characterization of the inner and outer surfaces of the bubble shell, the explosion center, and the initial magnetic field ($\mathbf{B}^0$). This model is well suited to exploring the impact of the choice of shell shape and explosion center location on predictions of the Local Bubble shell contribution to the Faraday RM and the synchrotron polarized emission.

2.2 Application to the shell of the Local Bubble

To predict the contribution from the thick shell of the Local Bubble to the Faraday RM and polarized synchrotron emission, we inform our theoretical model with observational data and constraints found in the literature. Firstly, the strength and direction of the initial magnetic field (before the explosion) is set by fixing the three parameters (B^0, $l_{\mathbf{B}^0}$, $b_{\mathbf{B}^0}$), where B^0 is the amplitude and $l_{\mathbf{B}^0}$ and $b_{\mathbf{B}^0}$ are the Galactic longitude and latitude which fix the direction of $\mathbf{B}^0$. Secondly, the shapes of the inner and outer surfaces of the shell is given as input. Thirdly, the location of the effective explosion center is set by setting its Cartesian coordinates (x_c, y_c, z_c) in the (Galactic) Heliocentric reference frame where the Galactic center (longitude 0) is toward positive x and the Galactic North pole is toward positive z. Using our analytical model, the three above inputs (six parameters plus inner and outer surfaces) make it possible to estimate the magnetic field anywhere in the shell of the Local Bubble. Finally, to produce maps of the Faraday RM and of the synchrotron Stokes parameters Q and U, we adopt models for the thermal electron density, for the cosmic-ray electron (CRE) density, and for the energy-spectrum of the CRE.

In this study, we are exploring the effects from the choice of the geometry of the Local Bubble

shell and of the location of the explosion center. We construct six scenarios that implement variations of the model. The first type consists of spherical bubble shells (with constant thickness). Their names start with SC. For the second type, the bubble shells have their inner surface directly corresponding to the model derived by [9] from the 3D dust density map of [21] with a maximum multipole $l_{\rm max} = 6$ (i.e. $r_{\rm inner}^{\ell_{\rm max}=6}$), see Figure 1. Their names start with a D. For this second type, we consider the case where the shell thickness (as measured radially from a certain position) is constant (named DC) and the case where it varies (named DD). For this latter case, we adopt the outer surface of the shell ($r_{\rm outer}^{\ell_{\rm max}=6}$) as determined in [20], also from the same 3D dust map. To fix the center and the inner radius of the sphere for the spherical bubble-shell scenarios, we choose to fit a sphere to the 3D data points drawn from $r_{\rm inner}^{\ell_{\rm max}=6}$. As such, our spherical model for the Local Bubble is also derived from 3D dust data. In the Heliocentric Cartesian coordinate system, the center of the sphere is found at $(x_{\rm sph},\, y_{\rm sph},\, z_{\rm sph}) = (-24.8,\, -32.6,\, -23.3)$ pc and its radius is $R_{\rm sph} = 216.7$ pc. For the constant thickness of the shell, we adopt the value of $\Delta = 35$ pc, in agreement with the model of [5]. For the case named DC we choose $(x_{\rm sph},\, y_{\rm sph},\, z_{\rm sph})$ as the point from which the shell thickness, as measured radially, is constant.

Relying on a model that assumes no thickness for the shell of the Local Bubble, constraints on the initial magnetic field orientation and on the position of the explosion center were obtained in [9] through a maximum-likelihood analysis of the Galactic polar caps of the dust polarized emission measured by the *Planck* satellite at 353 GHz. That analysis did not lead to constraints on the amplitude of the magnetic field as dust polarization is not directly sensitive to it. We consider their best-fit parameter values for the direction of $\mathbf{B}^0$: $(l_{\mathbf{B}^0},\, b_{\mathbf{B}^0}) = (73^\circ,\, 17^\circ)$. For the strength of the initial magnetic field (B^0) we consider a value of 3 μG which is close to the best-fit value obtained in [5] for their spherical bubble. For the locations of the explosion center we consider both, the solution obtained in [9]: $(x_c^{\rm P20},\, y_c^{\rm P20},\, z_c^{\rm P20}) = (23,\, -34,\, -122)$ pc and the center of the sphere that fits $r_{\rm inner}^{\ell_{\rm max}=6}$. The third letter of our scenarios' names indicates this choice. The letter O corresponds to explosion center at $(x_{\rm sph},\, y_{\rm sph},\, z_{\rm sph})$ and letter A corresponds to explosion center at $(x_c^{\rm P20},\, y_c^{\rm P20},\, z_c^{\rm P20})$.

For the homogeneous initial thermal-electron density, we adopt the value of $n_e = 0.015\,{\rm cm}^{-3}$ [22]. We consider that the thermal electron density is enhanced in the shell of the Local Bubble, according to the displacement field (see [20] for details). For the CRE, we consider the simplified assumption that they follow a power-law energy distribution with a spectral index of 3 and adopt the uniform density of $n_{10} = 1.2 \times 10^{-23}{\rm cm}^{-3}{\rm eV}^{-1}$, which was obtained for 10 GeV electrons outside the heliosphere [4]. Here, we consider that the CRE density is not perturbed by the formation of the Local Bubble.

3. Results

Using our analytical model, we estimate the contribution from the shell of the Local Bubble to the Faraday RM and the Stokes parameters Q and U of the polarized synchrotron emission for the six scenarios constructed above. In Figure 2 we show the full-sky map produced using an HEALPix angular tesselation with $N_{\rm side} = 64$ [23], and using 100 steps through the shell to compute the line-of-sight integral of the observables. Given our model assumptions, the RM maps scale with $n_e\, B^0$ while the Q and U maps scale with $n_{10}\, (B^0)^2$. It is observed that the convoluted

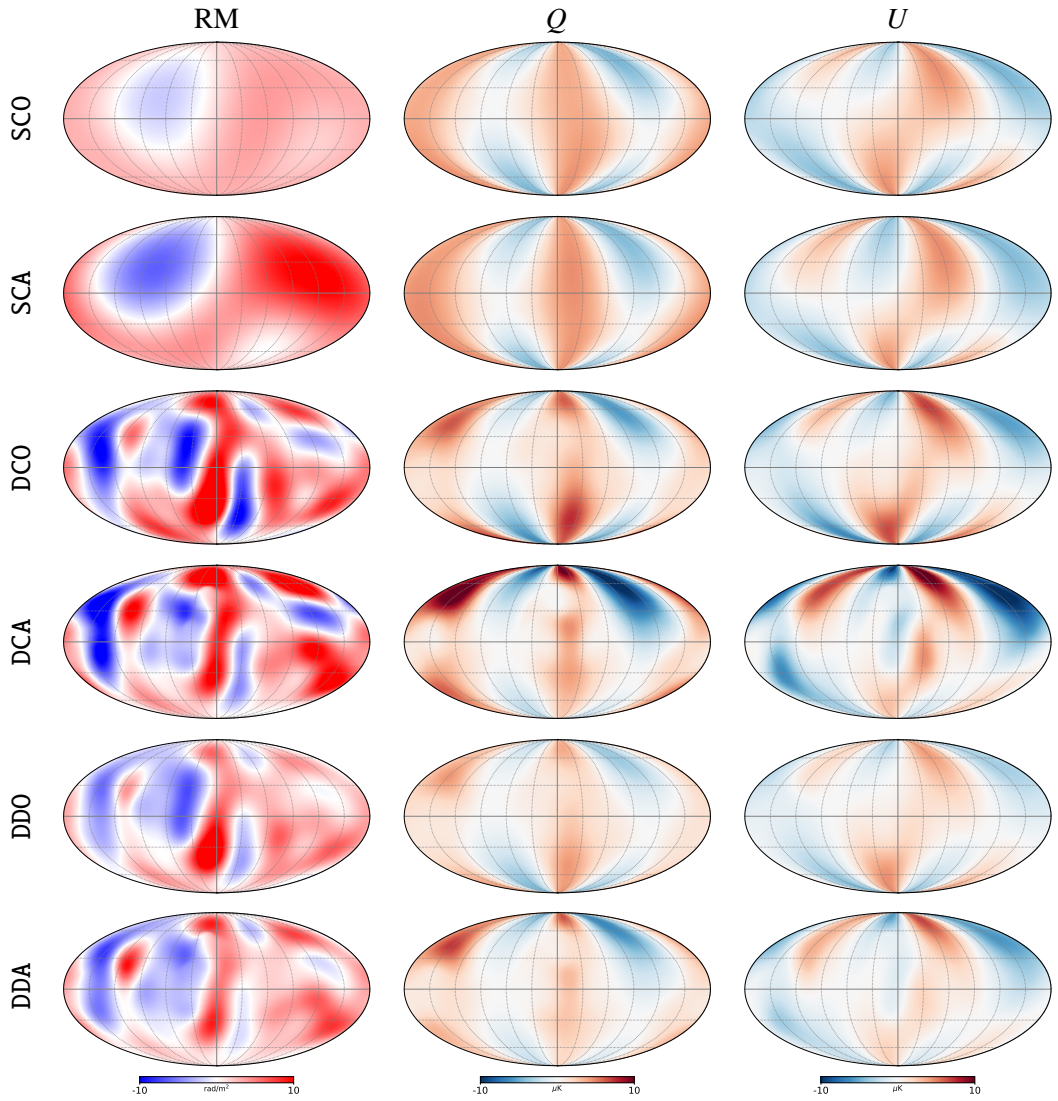

Figure 2: Mollweide projection of the full-sky maps of the contributions from the shell of the Local Bubble to the RM, Q, and U signal (from left to right) as predicted for our different scenarios (rows). Maps are given in Galactic coordinates with the Galactic center at the center of the maps, Galactic longitude increases to the left and the Galactic North pole is at the top. Color scales are shared in columns. They range from -10 to 10 rad/m^2 for the RM maps and from -10 to 10 μK for Q and U maps.

shape of the Local Bubble shell leads to a certain number of anisotropies in the maps, the details of which depend on the shell shape, the choice of the explosion center and the thickness of the shell. This is true for both Faraday RM and synchrotron polarized emission. The morphology and exact position of these anisotropies in the sky also depend on ($l_{\mathbf{B}^0}$ and $b_{\mathbf{B}^0}$) (not shown in the figure). The substantial North-South asymmetry seen in the maps of the `DCA` and `DDA` cases as compared to `DCO` and `DDO` cases is due to the fact that in `A` cases, the explosion center is significantly further below the Galactic plane (-122 pc as compared to -23.3 pc). As a consequence, the amount of matter and magnetic field lines that have been swept up to the northern part of the Bubble is much larger than

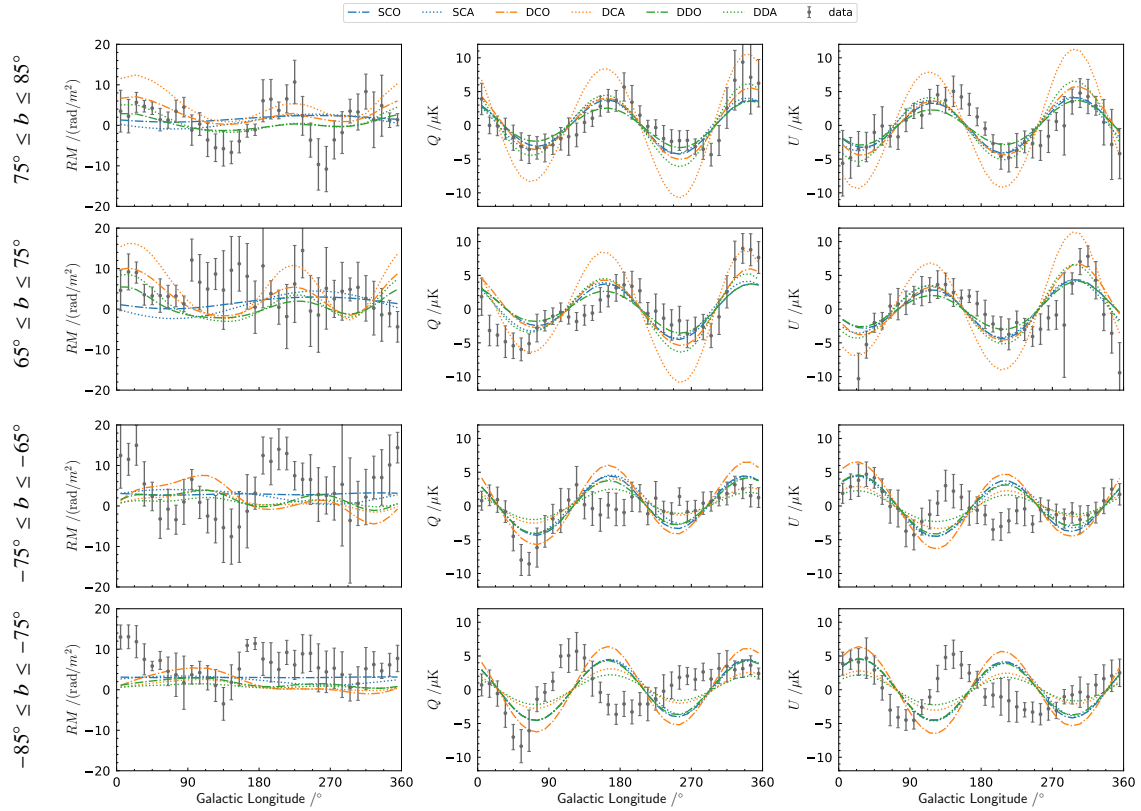

Figure 3: Longitude profiles for constant latitude stripes of 10° width for $|b| \in [65°, 85°]$, as described in the text. Predictions for the different scenarios for the Local Bubble magnetic field are shown as continuous lines according to the legend, for the RM, Q, and U signal (from left to right). For reference, observational data is also shown as gray points with symmetric errorbars.

to the South. Thus, we find that shell geometry and the location of the explosion center are decisive in assessing in details the shell's contribution to polarization observables.

The comparison with the model predictions between them and with data is illustrated in Figure 3 using longitude profiles for several stripes of constant latitudes. We consider latitude stripes of width of 10° with centers at 70° and 80°, both in the northern and southern hemispheres. The longitude profiles are constructed by taking the average of the model predictions, or observations, in longitude bins of 10° width. The error bars correspond to the standard deviation of the observation in each bin. It relates to the scatter in the data that primarily results from small-scale fluctuations in the magnetized ISM, plus the source contribution for the RM. For this comparison, we use the RM data from [4] at $N_{\rm side} = 32$, and the synchrotron Q and U data at 30 GHz from *Planck* processed data by the `Commander` component separation method [24], smoothed at a resolution of 1.2°, and downgraded at $N_{\rm side} = 64$. We do not mask the data to build these longitude profiles which, as a result, include features such as the North polar spur (seen in Q and U profiles in $l \lesssim 90°$ and $55° < b < 75°$).

The model-dependent anisotropies seen in Figure 2 are also seen in the longitude profiles, in both the Faraday RM and synchrotron polarization maps. Here also, we see that the shape and

thickness of the Local Bubble shell, as well as the choice for the location of the explosion center, influence the number, morphology, and amplitude of the anisotropies.

When compared to observation, we see that the amplitude of the contribution from the Local Bubble shell to the RM is generally smaller than in the data. This might indicate that the Local Bubble shell is on average a subdominant component of the RM integrated over the full path length through our Galaxy. The significance of the discrepancy between our model predictions and the data is relatively low given the large uncertainties in RM data (see [20] for details). As such, it is difficult to make any statement on the significance of the Local Bubble shell contribution to the line-of-sight-integrated Faraday RM. On the other hand, we find that, at these high latitudes, the contribution from the thick shell of the Local Bubble to the synchrotron polarization reaches the same amplitude as the one in observation. In addition, we find that the different scenarios lead to the same phase for the sinusoidal variation of the signal with longitude. This is because we assume the same direction for $\mathbf{B}^0$. However, the different scenarios predict variations in the amplitude of this sinusoidal signal and even departure from a perfect sine function. These differences depend primarily on the assumed shape and thickness of the shell. Of course, the shell models cannot account for the entirety of the signal and its variations. However, we emphasize that we have not resorted to any minimization, which makes the agreement between model predictions and data particularly remarkable. The result of a fit would probably improve this agreement. Therefore, we consider the observed agreement as astrong indication that the thick shell of the Local Bubble could be a significant contributor to synchrotron polarized emission at high Galactic latitudes.

4. Conclusion

It has recently been suggested that the Local Bubble shell could be an important foreground in modeling the large-scale Galactic magnetic field using Faraday RM and polarized synchrotron emission. This came with a simple spherical model to describe the Local Bubble [5] while it is known that it has an irregular shape [9]. In this work, we use the new physical model we have developed [20] to describe the divergence-free magnetic field in the thick shells of irregularly shaped Galactic bubbles and consider realistic shapes for the Local Bubble shell that we derived from a 3D dust density map. This allows us to explore the impact of the shell geometry and of the center of explosion, which led to the formation of the Local Bubble, on the model predictions. We find that, deviating from the spherical model with a centered explosion center, the model predictions for the contributions to the Faraday RM and synchrotron polarization maps severely depend on the shape and thickness of the shell, and on the assumed center of explosion. In addition, using published values for all free parameters of our model, we confirm that, at high Galactic latitudes, the thick Local Bubble shell may indeed contribute substantially to the polarization signal.

In conclusion, while reinforcing the idea that the local bubble shell could be an important foreground to consider when constraining large-scale GMF models from Faraday RM and synchrotron polarized emission, our analysis further shows that the geometry of the local bubble shell and the exact location of the explosion center are key parameters for reproducing detailed features. Our analysis strongly motivates the inclusion of realistic models for the Local Bubble in large-scale GMF models and to perform a full exploration of the parameter space.

Acknowledgments

VP acknowledges funding from a Marie Curie Action of the European Union (grant agreement No. 101107047).

References

[1] A. Coleman, J. Eser, E. Mayotte, et al. 2023, *Astrop. Phys.* 147, 102794

[2] The Pierre Auger Collaboration 2024, *JCAP*, 01 (2024), 022

[3] T. R. Jaffe 2019, *Galaxies*, 7, 2, 52

[4] M. Unger & G. R. Farrar 2024, *ApJ*, 970, 95

[5] A. Korochkin, D. Semikoz & P. Tinyakov 2025, *A&A*, 693, A284

[6] D. P. Cox & R. J. Reynolds 1987, *ARA&A*, 25, 303

[7] R. Lallement, B. Y. Welsh, J. L. Vergely, et al. 2003, *A&A*, 411, 447

[8] W. Liu, M. Chiao, M. R. Collier, et al. 2017, *ApJ*, 834, 33

[9] V. Pelgrims, K. Ferrière, F. Boulanger, et al. 2020, *A&A*, 636, A17

[10] T. J. O'Neill, C. Zucker, A. A. Goodman & G. Edenhofer 2024, *ApJ*, 973, 136

[11] J. Maíz-Apellániz, 2001, *ApJ*, 560, L83

[12] D. Breitschwerdt, J. Feige, M. M. Schulreich, et al. 2016, *Nature*, 532, 73

[13] M. M. Schulreich, J. Feige & D. Breitschwerdt 2023, *A&A*, 680, A39

[14] C. Heiles 1998, in proceedings of *IAU Colloq. 166*, 506, 229–238

[15] J. L. Leroy 1999, *A&A*, 346, 955

[16] B. G. Andersson & S. B. Potter 2005, *MNRAS*, 356, 1088

[17] B. G. Andersson & S. B. Potter 2006, *ApJ*, 640, L51

[18] G. A. Gontcharov & A. V. Mosenkov 2019, *MNRAS*, 483, 299

[19] I. Medan & B. G. Andersson 2019, *ApJ*, 873, 87

[20] V. Pelgrims, M. Unger & I. C. Mariş 2024, *A&A submitted*, arXiv:2411.06277

[21] R. Lallement, C. Babusiaux, J. L. Vergely, et al. 2019, *A&A*, 625, A135

[22] S. K. Ocker, J. M. Cordes & S. Chatterjee 2020, *ApJ*, 897, 124

[23] K. M. Górski, E. Hivon, A. J. Banday, et al. 2005, *ApJ*, 622, 759

[24] Planck Collaboration IV. 2020, *A&A*, 641, A4